NUMERICAL MODELLING OF WATER SPRAY BARRIERS FOR DISPERSING DENSE GASES

R. N. MERONEY* and D. E. NEFF**

Fluid Mechanics and Wind Engineering Program, Department of Civil Engineering, Colorado State University, Fort Collins, CO 80523, U.S.A.

(Received in final form 27 July, 1984)

Abstract. A depth-integrated numerical model is used to calculate the behavior of heavy and cold gas clouds subjected to the diluting influence of a water spray curtain. The model includes the physics of a cold cloud heated by the ground which entrains moist air. Entrainment velocities are influenced by cloud stratification. Laboratory water-curtain trials are predicted accurately. The model reveals the influence of curtain placement, width of spray, spray strength and thermal effects on the efficacy of the water curtain to mitigate potential hazards.

List of Symbols

Symbol	*Definitions*	*Dimensions*
A_i	Intersection area between cloud and water spray.	$[L^2]$
B	Plume width scale predicted by slab program.	$[L]$
ΔB	Initial plume width scale used by slab program.	$[L]$
$\overline{C}_m$	Maximum average volumetric or mole fraction.	–
$\overline{C}_{mb}$	Maximum average volumetric or mole fraction before spray at spray intersection.	–
d_g	Conical water spray impact diameter with plume.	$[L]$
DP	Dilution parameter.	–
FD	Forced dilution factor.	–
H	Plume vertical scale.	$[L]$
L	Plume width.	$[L]$
L_s	Lateral spray nozzle separation.	$[L]$
LFL	Lower flamability length.	–
MF	Entrainment velocity water spray multiplication factor $g\Delta H/(\rho u_*^2)$.	–
N	Number of water spray nozzles.	–
p	Water pressure.	$[F/L^2]$
Q_0, Q_s	Volumetric source strength.	$[L^3/T]$
Q_e	Air volume entrainment rate.	$[L^3/T]$
Ri_*	Local plume Richardson number.	–
S	Distance to water spray line downwind of source.	$[L]$
ΔS	Downwind interval over which spray intersects plume.	$[L]$
SG	Specific gravity with respect to air at STP.	–
t_R	Source release time for finite volume releases.	$[T]$
T_a	Temperature ambient air.	[ ]
T_s	Temperature source gas.	[ ]
u	Wind speed.	$[L/T]$
u_g	Plume frontal velocity.	$[L/T]$

* Professor, Civil Engineering.
** Research Associate, Civil Engineering.

Boundary Layer Meteorology **31** (1985) 233–247. 0006–8314/85/0313–0233$02.55.

u_*	Friction velocity.	$[L/T]$
w_*	Convective velocity.	$[L/T]$
w_e	Entrainment velocity.	$[L/T]$
$(w_e)_{spray}$	Entrainment velocity induced by water spray.	$[L/T]$
x	Downwind distance.	$[L]$
Δx	Initial source length.	$[L]$
z_0	Surface roughness	$[L]$
ϕ	Relative humidity.	–

1. Introduction

Water spray curtains have been proposed as an effective means to mitigate the consequences of a release of heavy flammable gases into the atmosphere. The water spray curtain acts to entrain large quantities of air, producing rapid dilution of the dense plume.* Design procedures for such water barriers have been proposed by various authors based on simple two-dimensional analyses (McQuaid and Fitzpatrick 1981; Zalosh *et al.*, 1981). Models of the water-spray barrier/gas plume are examined in this paper. The models, which include three-dimensional, transient, and thermal effects, are compared to field and laboratory experiments, and then run to examine the influence of a number of adjustable parameters on the performance of a water-spray installation.

Semi-empirical theories of dilution by water-spray driven entrainment of air have been developed by Moore and Rees (1981). They predicted that a forced dilution factor, FD, is linearly dependent on the sum of entrainment from the turbulence in the wind and the water spray. Plume dilution became a simple function of downwind distance, assumed ratio of the air velocity in the water spray to the wind speed, and various entrainment constants. McQuaid and Fitzpatrick (1981) used a simple two-dimensional box-type model to predict water-spray barrier effects. In this model the water-spray barrier was replaced by a line source of air at the same location as the barrier, and the air was assumed to mix instantaneously with the plume, producing a sudden change in composition and geometry of the plume. McQuaid's model sees the plume as a series of slices, each of which behaves in the same way as the cloud. Beyond a certain location, his model assumes a transition to passive dispersion behavior predicted by empirical dispersion curves. Transient behavior and thermal effects were not considered. Zalosh *et al.* (1981) calculated water spray behavior with a two-dimensional elliptic numerical code. The gas motion was derived by a method similar to that of the TEACH-T computer code (Pun and Spalding, 1977) for turbulent, recirculating, two-dimensional flow fields. The droplet spray was coupled to this gas phase calculation by means of a particle-in-cell technique. The code could be modified to incorporate the influence of latent heat release due to water condensation and heat transfer; however, the results described by Zalosh *et al.* (1981) were for situations with adiabatic entrainment and no latent heat release. The model predicts streamlines, isotherms, and isopleths of concentration.

* The water spray acts to entrain air which may dilute the dangerous gases below their lower flammability limit (LFL). It does not contain or eliminate the flammable gases.

2. Numerical Models of Water-Curtain/Dense-Plume Systems

2.1. General

Models for dense-cloud dispersion are desired which produce the detailed nuances of behavior perceived during laboratory and field experiments. Three-dimensional calculations are very expensive of computer storage and time. Fortunately, when the flow situation is only weakly three dimensional so that some dimensions can be decoupled from the others, a set of simpler relations can be obtained by integrating the conservation equations. When the flow situation is steady and diffusion in one direction is weak with respect to advection, it is possible to integrate over a plume cross-section and calculate plume width, average height, and cross-section averaged velocities, concentrations, temperatures, and humidity. Such a 'box' type model is numerically very fast since the conservation equations reduce to a set of coupled ordinary differential equations. Alternatively, when vapor generation is transient, and there are opportunities for upwind flow, a set of coupled partial differential equations of only two dimensions and time can be created by integrating the conservation equations over just the depth. Such a 'shallow layer' or 'slab' type model provides information about time- and space-dependent cloud widths, heights, and depth-averaged velocities, concentrations, temperatures, and humidity. Modifications of two such programs to handle the presence of a water spray curtain are described below. (The reader is referred to detailed model descriptions found in other papers.) Similar models which might be modified in a like manner are summarized by Blackmore *et al.* (1982).

2.2. Numerical box model

Consider a dense cloud which is continuously released through a vertical rectangular area of width, L_0, and height, H_0, that undergoes a slumping motion during which L increases with time. As the cloud moves downwind, the cloud section mixes with ambient air, but maintains uniform properties internally at each downwind section. The lateral velocity is assumed to vary linearly from zero at the center to a maximum at the outer edge of the cloud. Such behaviour is sketched in Figure 1. Sketches of how the actual cloud is perceived to disperse are shown to the right of each box model sketch. Although the simplistic model may reproduce lateral cloud dimensions and maximum concentrations measured, it cannot correctly reproduce the actual lateral variation of height and concentration in space.

In this model, lateral spread rate of the cloud front is proportional to the excess hydrostatic head within the cloud. Dilution of the gas cloud is assumed to occur by entrainment across the upper surface and at the lateral edges as audited by a molar conservation equation. Longitudinal momentum and enthalpy are conserved in separate relations which use entrainment of ambient flow, surface drag, surface heat transfer, and condensation algorithms as required. The resulting four coupled ordinary differential equations were solved by a fourth-order Runga–Kutta scheme. Model details have been discussed by Meroney and Lohmeyer (1984). Meroney (1983), and Andreiev *et al.*

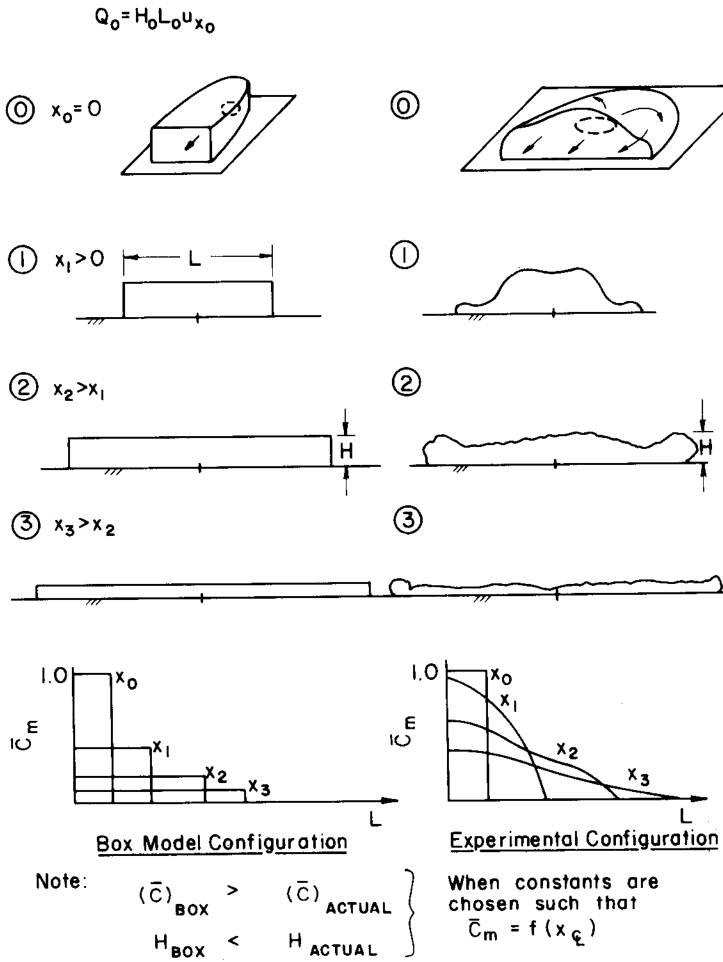

Fig. 1. Box-model plume behavior.

(1983). Model modifications to handle the mixing effects of a water spray curtain are discussed below.

2.3. Numerical slab model

The layer-averaged (slab) model solved the depth-averaged lateral and longitudinal momentum, mass continuity, concentration and enthalpy equations for longitudinally varying depth and width and cross-section averaged densities, temperatures, velocities, and concentrations. The model did not use the Boussinesq assumption, but implicitly made the hydrostatic pressure assumption. The partial differential equations were developed in a difference form using an implicit, second-upwind-difference, donor-cell approach. The difference equations were solved by the Thomas algorithm, and over the integration periods conserved 99.5% of the mass. Model details are described by Meroney and Lohmeyer (1982) and Meroney (1984).

2.4. Program modifications for water-spray curtains

Both numerical models normally use the concept of an entrainment velocity, w_e, across the upper cloud surface to mix the cloud with ambient air. The entrainment velocity is a semi-empirical function of boundary-layer and cloud variables such that,

$$w_e = f(u_g, u_*, w_*, \mathrm{Ri}_*) ,$$

where

u_g = plume frontal velocity,
u_* = friction velocity,
w_* = convective velocity, and
Ri_* = local plume Richardson number.

The presence of a water-spray barrier results in a local increase in entrainment rate. McQuaid and Fitzpatrick (1981) hypothesized a finite increase in local entrainment without specifying how the numbers would be related to nozzles used or their location; however, McQuaid (1975) derived a semi-empirical relationship for conical sprays which gives the rate of entrainment of air as a function of water flow, water pressure and size of spray. Of course, $(w_e)_{\text{spray}} = Q_e/A_i$, where Q_e is flux of air entrained and A_i is the area of intersection between cloud and spray. Heskestad *et al.* (1976) also predicted a range of entrainment rates in terms of water flow, spray type, spray angle and distance from the nozzle. Values of $(w_e)_{\text{spray}}$ ranged from 5.0 to 34.0 m s^{-1} when nozzle diameters ranged from 1 to 25 mm, spray angles ranged from 30 to 130°, and cloud intersection distance varied from 0.25 to 4.0 m.

Water spray entrainment can be included in the two models by either using a multiplicative factor with the normal entrainment rate, i.e., $(w_e)_{\text{total}} = MF \times w_e$, or an additive factor, i.e., $(w_e)_{\text{total}} = w_e + (w_e)_{\text{spray}}$.* In addition, the area of interaction, A_i, is specified by the downwind interval, ΔS, over which the spray intersects the plume. To ensure good mixing, McQuaid (1977) suggested a minimum velocity of air in the spray ($w_e > 6$ m s^{-1}) at the plane where the spray meets the gas. In a 3 m s^{-1} wind, a typical level of entrainment due to mechanical mixing alone would be 0.2 m s^{-1}: hence, the multiplicative factors will range from 25 to 170.

The *MF* model permits some damping of the spray effect by the dense cloud stratification, but the additive model uses an entrained air velocity which relates to earlier spray models. The interval of spray interaction, ΔS, should relate to lateral nozzle separation, L_s, and impact circle diameter, d_g, by the equation $\Delta S = \pi d_g^2/(4L_s)$. The effective

* The additive factor approach must be considered more realistic: however, there are circumstances where a multiplicative methodology might be more convenient if shown to be nominally effective (i.e., the question would be: Is the *MF* approach good enough?).

entrained air velocity may be estimated from actual data from

$$(w_e)_{\text{spray}} = \frac{Q_s(T_a/T_s)(1 - \bar{C}_{\text{spray}}/\bar{C}_{\text{no spray}})}{\bar{C}_{\text{spray}} N(\pi d_g^2/4)},$$

and the multiplicative factor is then $MF = (w_e)_{\text{spray}}/w_e = ((w_e)_{\text{spray}}/(0.3u_*)$.

3. Comparison of Model Predictions with Laboratory Results

Results from a laboratory program to study water-spray curtain interaction with dense gas plumes were used to check the numerical models outlined above (Heskestad *et al.*, 1983). The wind-tunnel spray simulation was compared against field data in a separate test series (Meroney *et al.*, 1984). The experiments were carried out in the Environmental Wind Tunnel at Colorado State University. A 60 × 60 m diked area was simulated at a linear scale ratio of 1 : 100; hence, the model measured 60 × 60 cm. Figure 2 is a plan

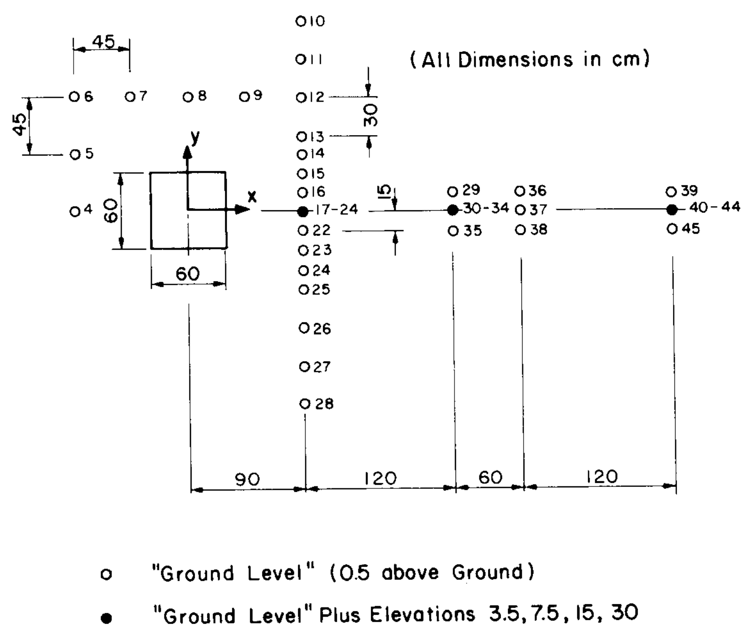

Fig. 2. CSU water spray curtain model experiments.

view of the model, together with the sampling grid used for the concentration measurements. The diked model was built into a turntable flush with the floor of the tunnel to allow variations in the relative wind direction.

Carbon dioxide at room temperature, with a small amount of ethane for detection (approximately 1%), was used as LNG-vapor simulant (specific gravity relative to STP air = 1.5). Samples were drawn through plastic tubing into syringes over a 5-min interval and subsequently analyzed with a flame-ionization detector in a gas chromatograph.

Spray nozzles used were manufactured by Spraco, Inc. and produce full cone sprays over the low pressures used. Heskestad *et al.* (1983) discuss the full range of configurations studied; however, the cases selected for comparison (Runs No. 62, 80, 134–138) positioned the nozzles 21 cm downwind of the diked area pointed 45° forward of downward from a height of 14.2 cm. Heskestad *et al.* (1983) inferred entrainment velocities equal to 0.791 m s^{-1} for Run 137, which implies a multiplicative factor, $MF = 116$.

The intention of the following calculations is to predict the postspray behavior of the dense gas plumes. Hence, experimental data were used to predict $(w_e)_{\text{spray}}$ by the manner suggested in the previous section, and the numerical model results are not a test of some empirical model for $(w_e)_{\text{spray}}$ based on water pressure, nozzle size and spacing.

Figure 3 indicates concentration decay rates downwind of the model dike with and without sprays. In this figure, the box model predictions for different effective multiplicative factors are compared with data. In each case, the multiplicative factor adjustment

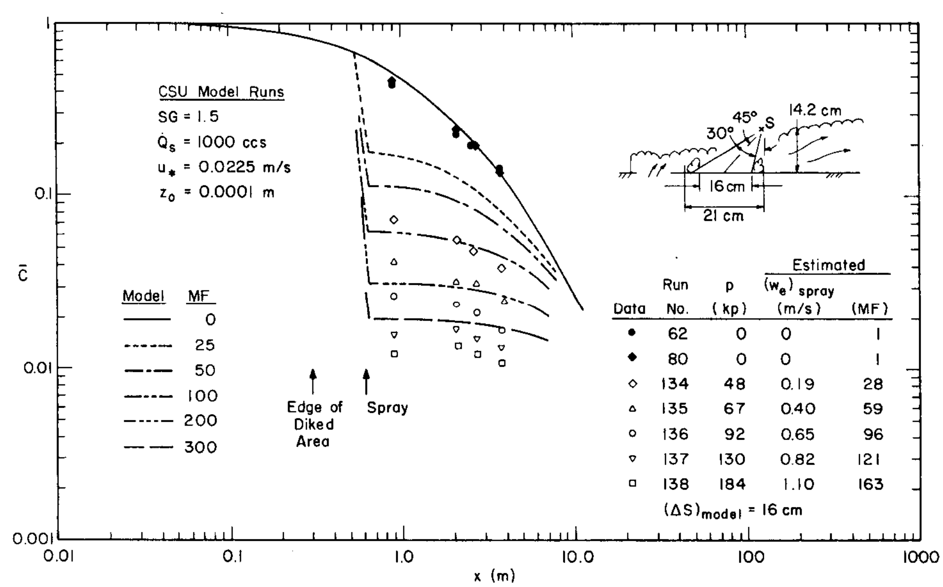

Fig. 3. Methane equivalent concentrations versus downwind distance, compared with box model using multiplicative factor.

to entrainment rate underpredicts the spray effect. Since the Richardson number is of the order of 35 before spray mixing, the damping effect of the stratification during calculations is indeed significant. The slab model with multiplicative factor adjustments also underpredicted spray mixing.

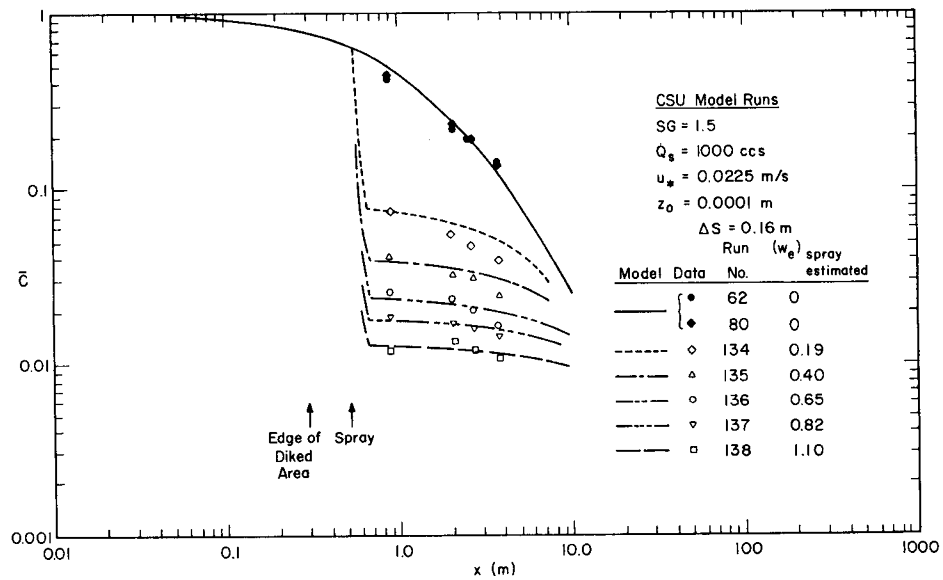

Fig. 4. Methane equivalent concentrations versus downwind distance, compared with box model using specified entrainment velocity.

Use of an additive factor is considered in Figure 4. Model predictions reproduced the dilution observed. At the lower entrainment velocities, concentrations predicted by the box model for distances downwind of the spray location did not decay quite as fast as observed. Figure 5 displays the influence of varying wind speed but retaining the same

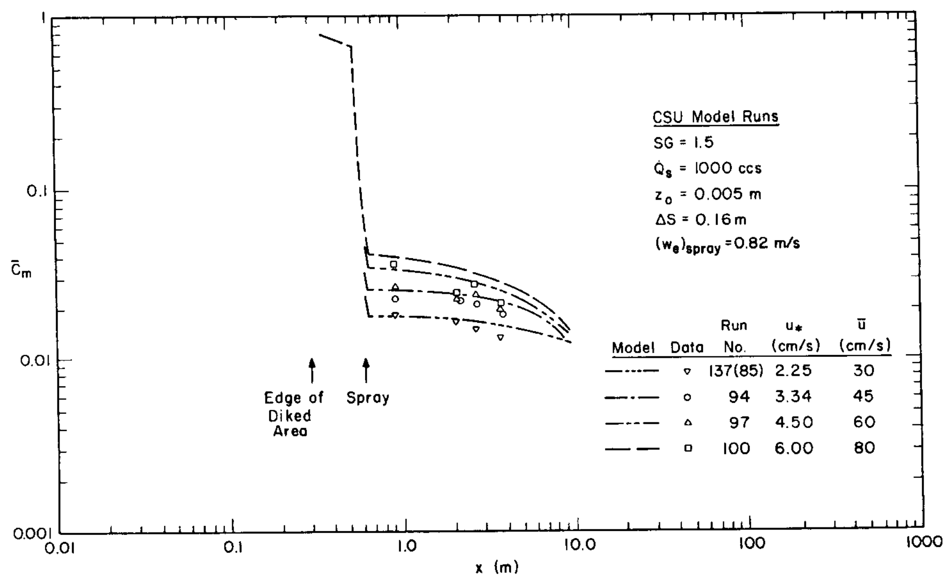

Fig. 5. Methane equivalent concentrations versus downwind distance, velocity varying from 30 to 80 cm s^{-1}, compared with box model using specified entrainment velocity.

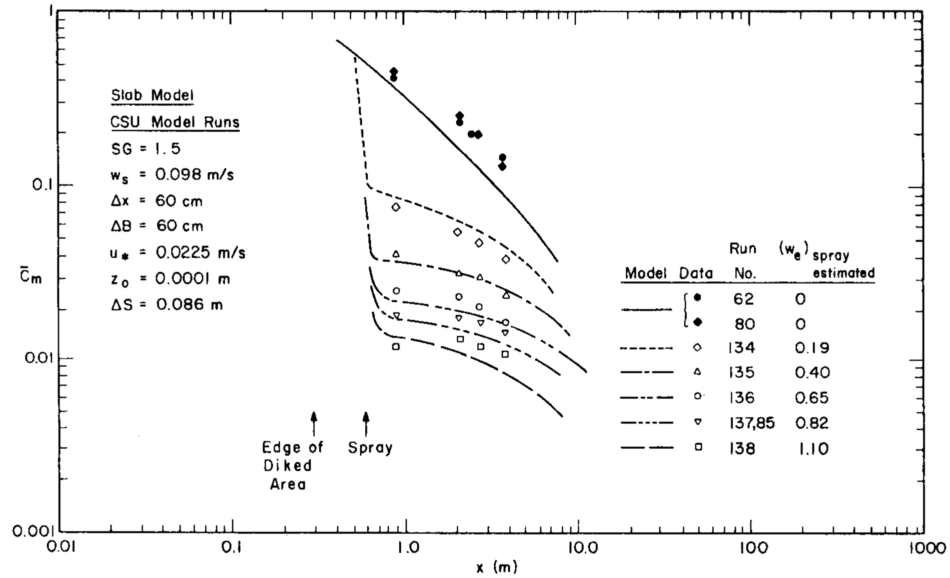

Fig. 6. Methane equivalent concentrations versus downwind distance, compared with slab model using specified entrainment velocity.

spray curtain entrainment velocity (i.e., the same water pressure). Again the model satisfactorily reproduces the experimental behavior. Slab model calculations using the additive entrainment velocity also mixed at rates observed during the experiments (Figure 6). In addition, the slab model reproduced post spray curtain concentration decay rates.

In the experiment, the water sprays surrounded the dike rather than extending in a downwind line; the agreement between model and data is therefore quite satisfactory; hence, one can make comparative design calculations with confidence.

4. Plume Response for Various Water-Spray Barrier Variations

4.1. General

The conditions selected for design variations are equivalent to those observed during Run No. 8 of the Burro Liquid Natural Gas (LNG) spills performed at China Lake, California, by Koopman *et al.* (1982). The source gas was emitted from LNG spilled at a rate of 15 m^3 min^{-1} on a small pond. The weather was slightly stable and wind speeds were about 2 m s^{-1} and decreasing. The no-spray Burro No. 8 data plotted are maximum ground-level concentrations detected at plume centerline locations. Since the plume showed tendencies to bifurcate and elevate, the slab model is only a crude estimate of total plume behavior. Bifurcation was a joint result of heating, terrain slope, and wind unsteadiness. No water spray curtain tests were performed; however, calculations to show the effect of hypothetical spray curtains are interesting. The effect of spray barrier location, spray entrainment rate, dual spray curtains, heat transfer and humidity, and wind speed are examined below. Calculations were performed with the additive entrainment velocity versions of both the box and slab models.

4.2. Effects of spray barrier location

In these calculations, only the location of the spray curtain was changed: from 25 to 55 to 120 m downwind of the spill center. Figure 7 displays box model predictions where

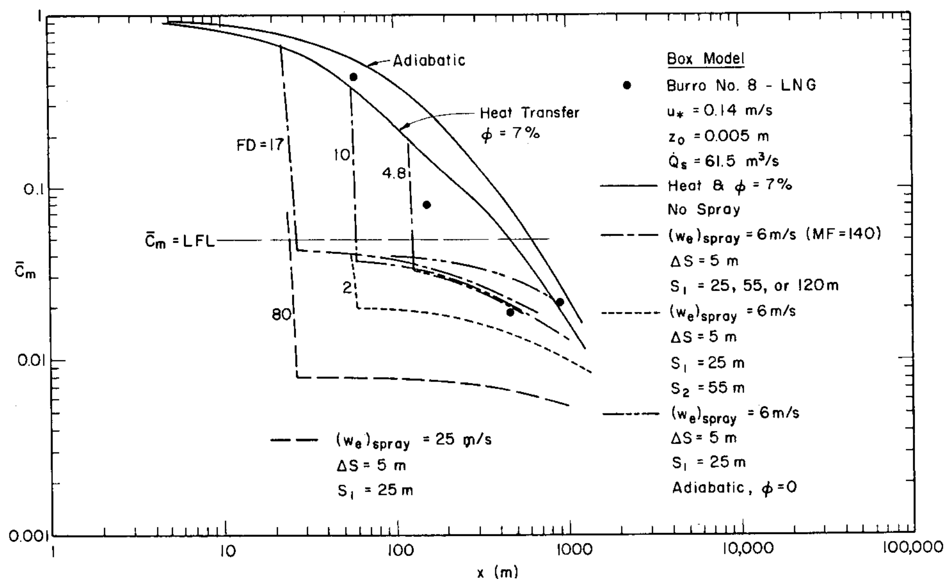

Fig. 7. Burro No. 8 LNG spill conditions, perturbed by various spray curtain arrangements as calculated by a Box model with specified entrainment velocity.

it is noted that the forced dilution factor, $FD = \overline{C}_{\text{no spray}}/\overline{C}_{\text{spray}}$, decreases with increased distance between spray curtain and source. The post-spray concentrations are very similar with slightly lower concentrations when the spray is farther downwind. The magnitude of the reduction in concentrations when the barrier is farther from the source is not large and any advantage would be outweighed by the greatly increased water consumption as spray curtain width increases over the wider plume.

4.3. Effects of spray entrainment rate

Calculations were performed for the CSU water spray tests considered earlier over a five-fold range of spray entrainment velocity (see Figures 4 and 6). Given a constant location, wind speed, and plume width, increased entrainment velocities result in proportional increases in forced dilution factor, *FD*.

4.4. Effects of dual spray barriers

The diluting effect of two spray barriers operating such that $w_e = 6\ \mathrm{m\ s^{-1}}$ and located 25 and 55 m downwind of the spill site are shown in Figure 7. The net effect of two such barriers seems to be very close to the effect expected from one barrier with $w_e = 12\ \mathrm{m\ s^{-1}}$. Again the second barrier must interact over a wider plume; hence, greater water consumption may occur.

4.5. Effects of heat transfer and humidity

When a plume's negative buoyancy is due to temperature, it loses stratification as surface heat transfer and water condensation destroy its buoyancy. Consider the case of a cold adiabatic plume interacting with the water spray without humidity effects in Figure 7. The spray positioned at 25 m initially dilutes the plume in the same manner as before, but since the negative buoyancy is conserved, further mixing is suppressed. Indeed slab model calculations suggest that curtain mixing is more effective when the negative buoyancy is lost by heat transfer (Figure 8).

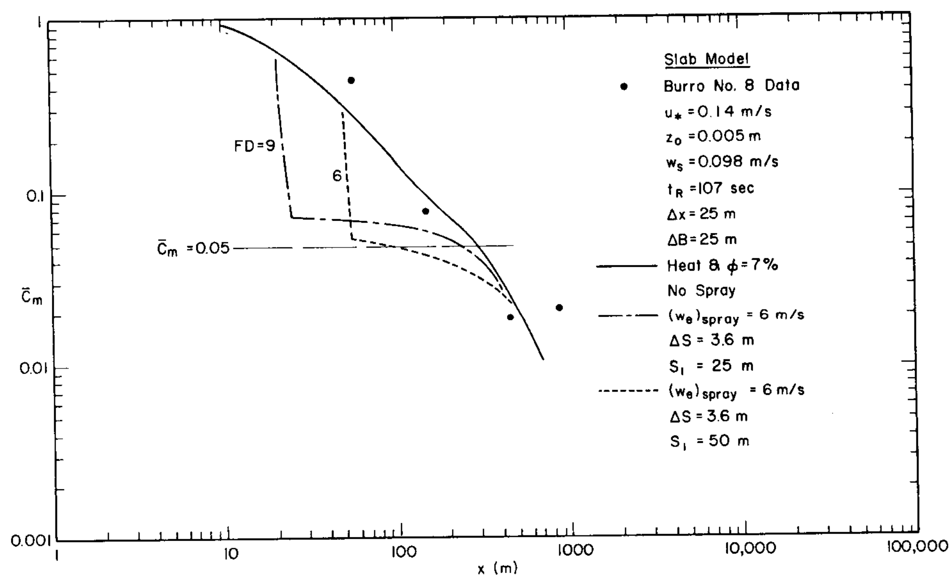

Fig. 8. Burro No. 8 LNG spill conditions, perturbed by various spray curtain arrangements as calculated by a slab model with specified entrainment velocity.

4.6. Effects of wind speed

Increased wind speed advects the gas plume through the spray zone more quickly. Figure 9 shows how the box model predicts that the *FD* factor decreases from 17 to 8.4 as the wind speed increases from 2 to $6\ \mathrm{m\ s^{-1}}$.

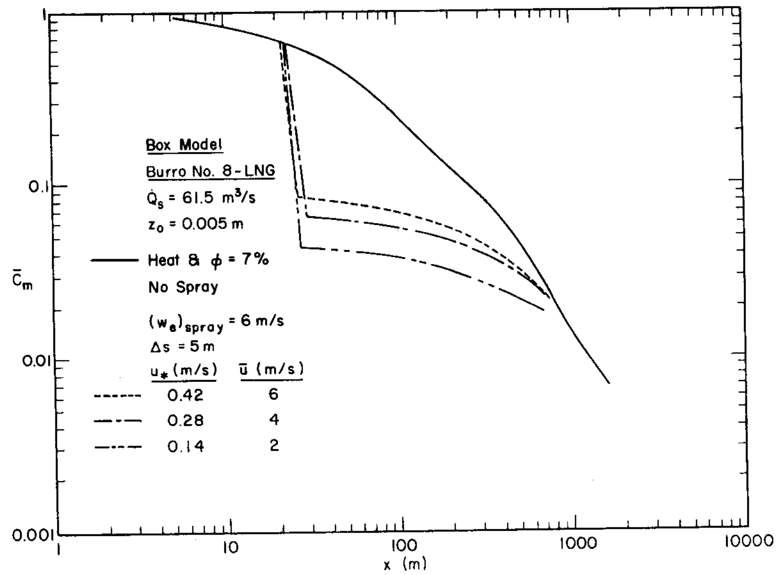

Fig. 9. Burro No. 8 LNG spill conditions, perturbed by various spray curtain arrangements as calculated by a box model with specified entrainment velocity.

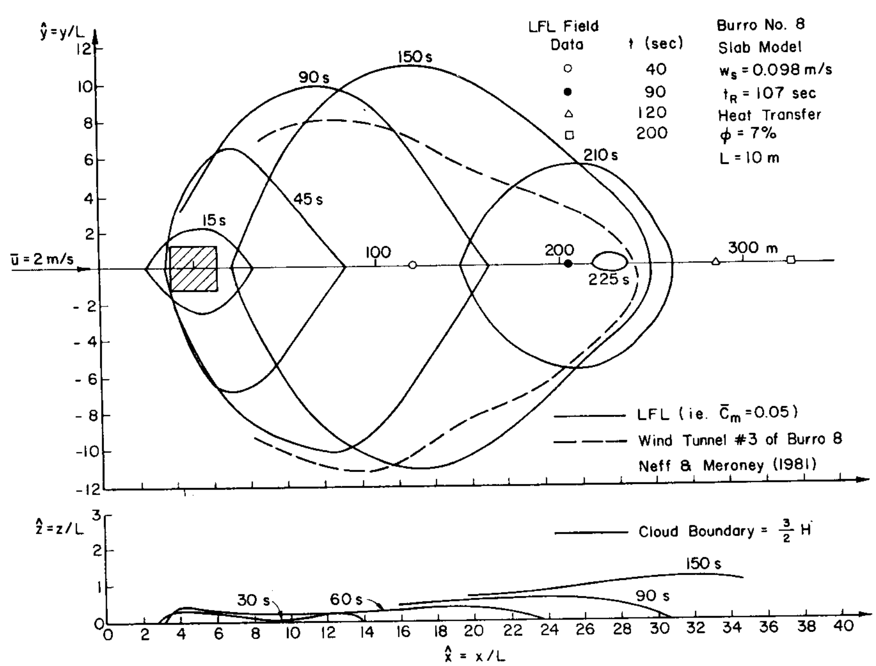

Fig. 10. Burro No. 8 LNG spill no spray conditions, plan view and vertical section.

4.7. Effect of water curtains on plume structure

Figure 10 displays slab model predictions of the ground-level regions where concentrations exceed the lower flammability limit (LFL) during the transient lifetime of the Burro No. 8 spill of LNG. The zone is instantaneously rather dish-shaped and very flat. The wind convects flammable gases nearly 300 m downwind. A vertical section of the plume displays the total vertical extent of each cloud versus time. (LFL) isopleths are not included on the vertical section since after a water spray (Figure 11), the isopleth sections disappear entirely. Consider the effects of a water curtain placed 55 m downwind of the spill, entraining air at 6 m s^{-1} as shown in Figure 11. The longitudinal extent of the plume average LFL isopleth is dramatically cut off at less than 100 m, but the characteristic plume height increases sevenfold. The beneficial effects of such a spray barrier are obvious.

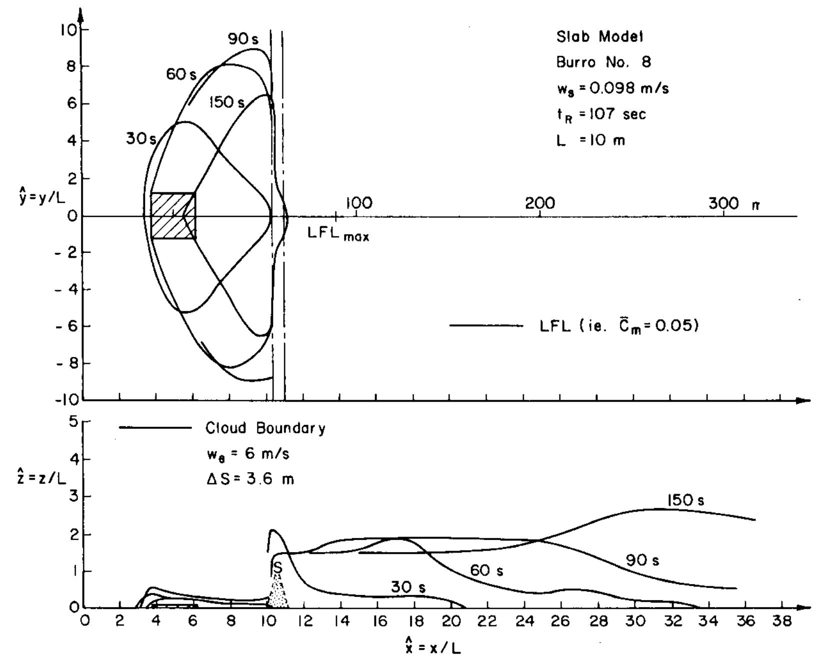

Fig. 11. Burro No. 8 LNG spill spray conditions, plan view and vertical section.

5. Summary

Variations in curtain position, spray entrainment velocity, wind speed, and source conditions resulted in a wide range of spray curtain performance as indicated by the forced dilution factor, *FD*. Despite the multiplicity of possible combinations of these variables, the results can be expressed in term of a forced dilution factor, *FD*, driven by an input dilution parameter, *DP*. When the calculated values for *FD* are plotted versus

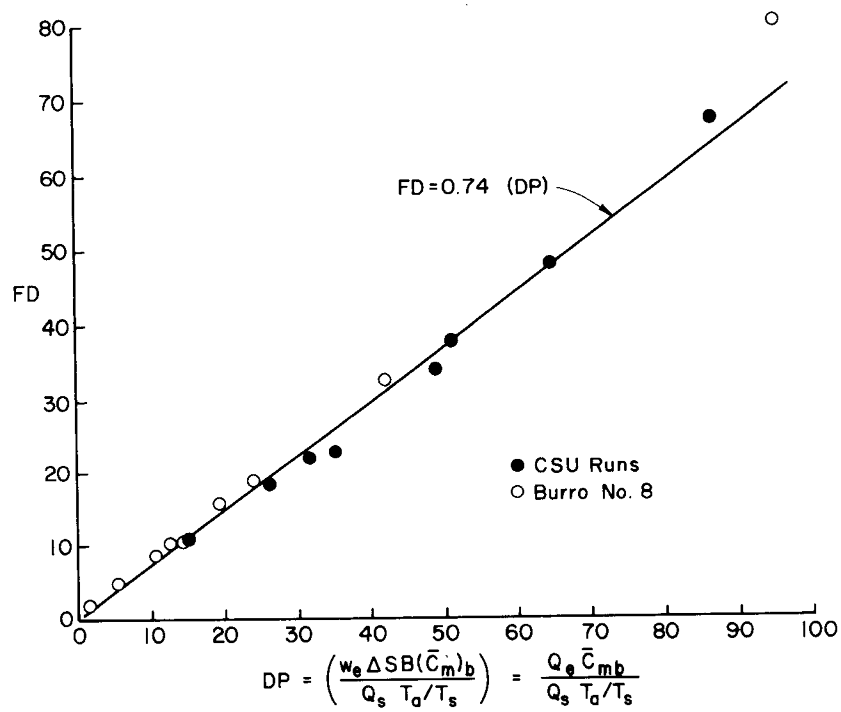

Fig. 12. Forced dilution factor versus dilution parameter.

a dilution parameter, $DP = Q_e \overline{C}_b T_s/(Q_s T_a)$, as shown in Figure 12 a nearly linear relation is observed, i.e.,

$$FD = 0.74(DP)\,.$$

Based on the calculation of $(w_e)_{\text{spray}}$ from experimental dilution data from the laboratory experiments, one should expect $FD = DP + 1$. The value used for plume width, B, is not the actual cloud width but a lateral cloud scale less than the true cloud width. If $B_{\text{actual}} \cong \frac{4}{3}B$, then $FD \cong DP$.

Since the numerical models used here were verified by measurements, they can be used with reasonable confidence. It is recognized that specifying spray performance in terms of a single parameter is somewhat simplistic; nonetheless, such values are available for sprays operating at low wind speeds, and the approach is appropriate at the present state of technology.

Acknowledgments

The author would like to thank the Gas Research Institute, U.S.A., and Factory Mutual Research, Inc. for their financial support. Discussions with Dr G. Heskestad, senior scientist, FMRC, were particularly helpful.

References

Andreiev, G., Neff, D. E., and Meroney, R. N.: 1983, *Heat Transfer Effects During Cold Dense Gas Dispersion*, Colorado State University, Civil Engineering Department Report CER83-84GA-DEN-RNM-3, for Gas Research Institute, Report GRI 83/00, 244 pp.

Blackmore, D. R., Herman, M. N., and Woodward, J. L.: 1982, 'Heavy Gas Dispersion Models', *J. Hazardous Materials* **6**, 107–128.

Heskestad, G., Kung, H. C., and Todtenkopf, N. F.: 1976, *Air Entrainment into Water Sprays and Spray Curtains*, American Society of Mechanical Engineers Paper 76-WA/FE-40, 11 p., plus Erratum, 18 January, 1977, 4 pp.

Heskestad, G., Meroney, R. N., Kothari, K. M., and Neff, D. E.: 1983, *Effectiveness of Water Spray Curtains in Dispersing LNG Vapor Clouds*, Proceedings American Gas Association Transmission Conference, Seattle, Washington, 2–4 May, 1983, 40 pp.

Koopman, R. P., Cederwall, R. T., Ermak, D. L., Goldwire, H. C. Jr., Hogan, W. J., McClure, J. W., McRae, T. G., Morgan, D. L., Rodean, H. C., and Shinn, J. H.: 1982, 'Analysis of Burro Series 40 m^3 LNG Spill Experiments', *J. Hazardous Materials* **6**, 43–84.

McQuaid, J.: 1975, 'Air Entrainment into Bounded Axisymmetric Sprays', *Proc. Inst. Mech. Eng.* **189**, 197–202.

McQuaid, J.: 1977, *The Design of Water-Spray Barriers for Chemical Plants*, 2nd International Loss Preventive Symposium, Heidelberg, pp. 511–518, DECHEMA, Frankfurt.

McQuaid, J. and Fitzpatrick, R. D.: 1981, *The Uses and Limitations of Water-Spray Barriers*, Northwestern Branch Symposium Papers 1981, No. 5, Institution of Chemical Engineers, Manchester, U. K., pp. 1.1.–1.13.

Meroney, R. N.: 1984, 'Transient Characteristics of Dense Gas Dispersion, Part I: A Depth-averaged Numerical Model', *J. Hazardous Materials*, **9**, 139–157.

Meroney, R. N. and Lohmeyer, A.: 1984, 'Prediction of Propane Cloud Prediction of Propane Cloud Dispersion by a Wind-Tunnel-Data Calibrated Box Model', *J. Hazardous Materials* **8**, 205–221.

Meroney, R. N., Neff, D. E., and Heskestad, G.: 1984, 'Wind-Tunnel Simulation of a U.K. Health and Safety Executive Water Spray Curtain Dense Gas Dispersion Test', *Boundary-Layer Meteorol.* **28**, 107–119.

Moore, P. A. C. and Rees, W. D.: 1981, *Forced Dispersion of Gases by Water and Steam*, North Western Branch Symposium Papers, No. 5, Institution of Chemical Engineers, Manchester, U.K., pp. 4.1–4.14.

Pun, W. M. and Spalding, D. B.: 1977, *A General Computer Program for Two-Dimensional Elliptic Flows*, HTS/76/2, Imperial College of Science and Technology, Mechanical Engineering Department, LLondon, U.K.

Zalosh, R. G., and Alpert, R. L., and Heskestad, G.: 1981, *Dispersal of LNG Vapor Clouds with Water Spray Curtains*, North Western Branch Symposium Papers, No. 5, Institution of Chemical Engineers, Manchester, U.K., pp. 3.1–3.17.